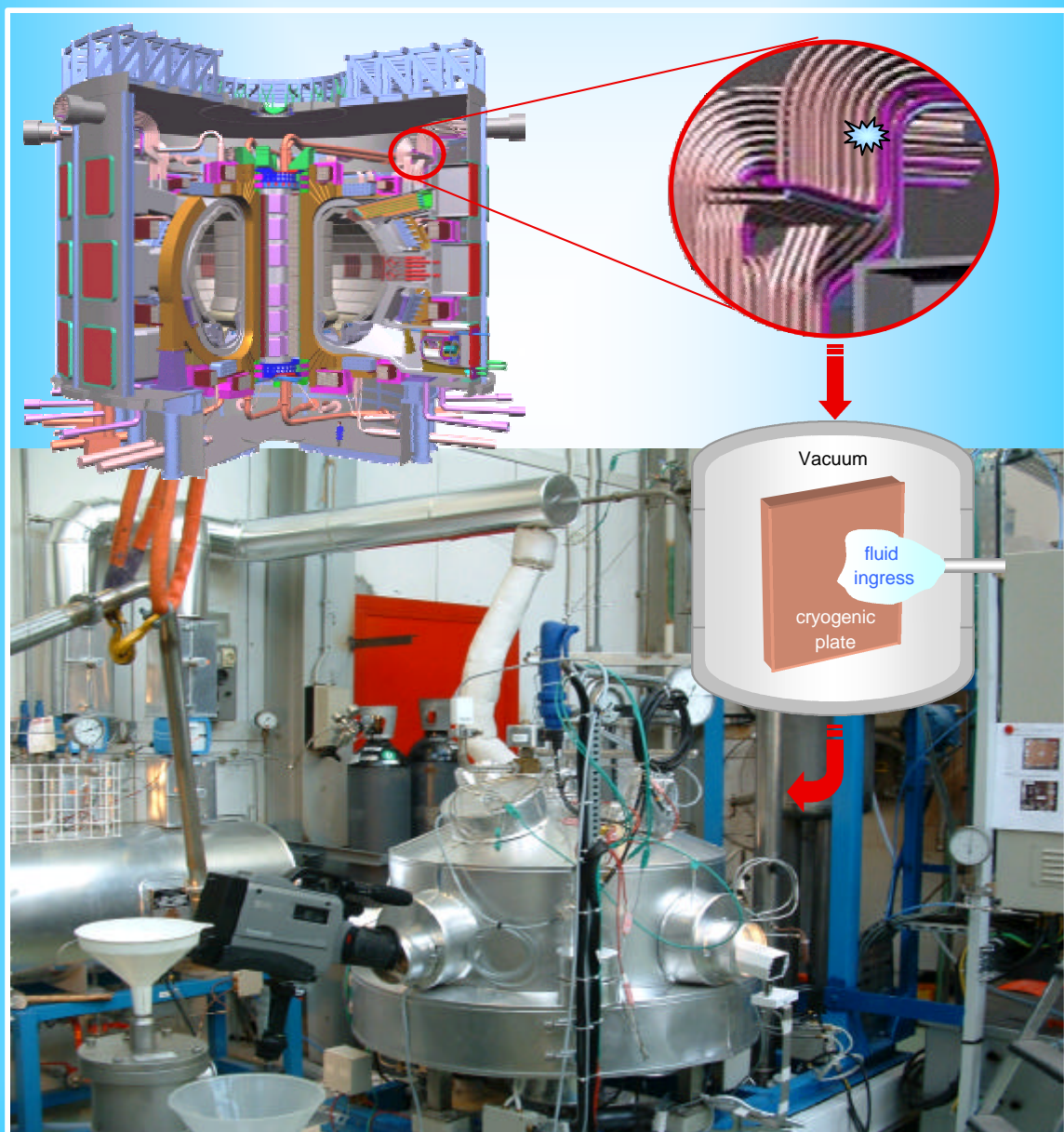# FUSION TECHNOLOGY

Annual Report of the Association EURATOM/CEA 2002

Compiled by : Ph. MAGAUD and F. Le VAGUERES

Vacuum

fluid ingress

cryogenic plate

CONTENTS

Plasma Facing Components

Remote Handling

Magnet Structure

Tritium Breeding and Materials

Breeding Blanket

Water Cooled Lithium Lead (WCLL) blanket

Helium Cooled Pebble Bed (HCPB) blanket

Helium Cooled Lithium Lead (HCLL) blanket

Structural materials development

Reduced Activation Ferritic Martensitic (RAFM) steels

Advanced materials

Neutron source

Safety and Environment

System Studies

Power Plant Conceptual Studies (PPCS)

Socio-economic studies

JET Technology

Physics Integration

Diagnostics

Vessel/In-Vessel

Plasma Facing Components

Remote Handling

Safety and Environment

Physics Integration

Diagnostics

Vessel/In-Vessel

Plasma Facing Components

Remote Handling

Tritium Breeding and Materials

Breeding Blanket

Materials development

Structural materials

Fuel cycle

Safety and Environment

System studies

Task Title: CRITICAL HEAT FLUX TESTING AND FATIGUE TESTING OF CFC MONOBLOCKS
200 kW electron beam gun test

INTRODUCTION

In ITER, the vertical target (VT) of the divertor consists in an assembly of 18 units. These units have a poloidal, toroidal and radial length of about 1400, 23 and 140 mm, respectively. The lower part consists in a straight CFC monoblock.

Both thermal fatigue and critical heat flux (CHF) limits are key issues as far as design of the element is concerned.

Therefore an experimental assessment of the thermal behaviour under cycling loads and under critical heat flux experiments of such component is an essential key to demonstrate the validity of the selected design solution.

Finally the need to reduce the cost of ITER - then of the divertor component- requires to investigate the possibility to increase the width of the VT from the present 23 mm to the highest possible value in order to reduce the overall number of toroidal VT units.

2002 ACTIVITIES

A high heat flux testing campaign dedicated to such issues, based on fatigue cycling and critical heat flux detection on straight monoblocks was performed on FE200 in the period july/august 2002 [1], [2], [3].

TEST SECTIONS

A total of 10 straight CFC NB31 monoblocks with 3 different width (23, 28, 33 mm) was manufactured to investigate width effect on fatigue behaviour and critical heat flux limits.

All of them have the following common features:

- one cooling channel of a CuCrZr Copper alloy tube;
- a twisted tape insert (twist ratio 2) made of OFHC Copper;
- 3 thermocouples implemented into the NB31 armour.

Table 1, left column summarizes the main features of the monoblocks. Note that AL28 has a 8mm thick NB31 armour instead of 3 mm for the 9 other monoblocks, this is aimed at investigating the possible effect of the armour thickness on the critical heat flux limit. AA33 is equipped with a CuCrZr tube of 12 mm internal diameter instead of 10 mm for the 9 other monoblocks, this is aimed at investigating the effect of the tube diameter on the critical heat flux limit for the largest tubes.

INFRARED EXAMINATION

The 10 samples were characterized on SATIR test bed, huge defects with DTref higher than 15°C were detected. Compilation of the measurements is given on figure 1 Nevertheless, due to the different width of the components, choice of reference has a great impact on the measurements an interpretation of the DTref values has to be moderated.
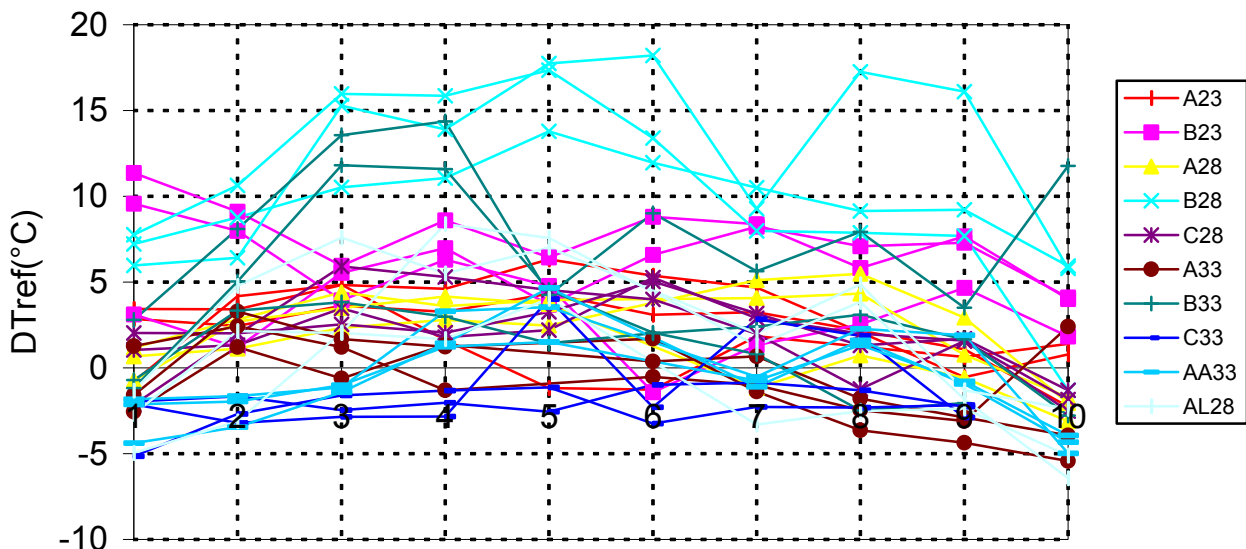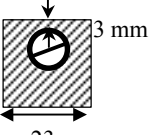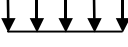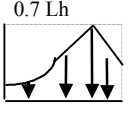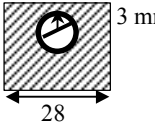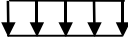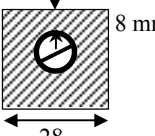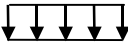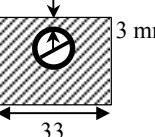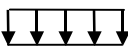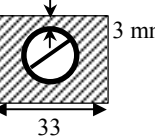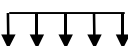
Figure 1 : Compilation of measured DTref on SATIR test bed for the 10 monoblocks

Table 1 : Summary of CHF tests results

Geometry and transversal incident flux profile	Longitudinal incident flux profile	Lh (m)	P (Mpa)	Tin (°C)	Tsat-Tout (°C)	V (m/s)	Power (kW)	Max.AHF (MW/m²)	FE WCHF (MW/m²)	FE Peaking Factor	Shot Number
07/02 : A23/B23 Material : NB31 + CuCrZr 3 mm 23 ID/OD 10/12 Eng. Pf = 2.3	Lh / 0.7 Lh / Fmax= 2.83 F̄	0,1 0,1 0,2	34,3 34,2 34,1	119,7 119,8 114,3	102,9 103,0 121,0	11,9 11,9 6,0	51,8 50,9 57,5	22,5 22,1 34,3	38,4 38,1 29,3	1,55 1,55 1,55	2601 2602 2627
07/02 : A28/B28/C28 Material : NB31 + CuCrZr 3 mm 28 ID/OD 10/12 Eng. Pf = 2.8	Lh	0,1 0,1 0,1	34,1 34,3 34,3	119,7 119,8 119,7	95,9 101,2 98,0	11,8 11,7 11,8	69,6 55,8 67,7	24,9 19,9 24,2	36,1 37,3 36,6	1,6 1,6 1,6	2605 2609 2611
07/02 : AL28 Material : NB31 + CuCrZr 8 mm 28 ID/OD 10/12 Eng. Pf = 2.8	Lh	0,1 0,1	33,7 33,5	119,8 109,9	98,0 98,8	5,1 3,3	54,1 50,0	19,3 17,9	23,3 18,7	1,75 1,75	2625 2626
07/02 : A33/B33/C33 Material : NB31 + CuCrZr 3 mm 33 ID/OD 10/12 Eng. Pf = 3.3	Lh	0,1 0,1 0,1	34,3 34,2 34,1	119,9 119,7 119,7	98,7 101,6 97,8	11,8 11,8 11,8	64,3 55,6 66,5	19,5 16,8 20,2	36,8 37,5 36,6	1,64 1,64 1,64	2606 2621 2620
07/02 : AA33 Material : NB31 + CuCrZr 3 mm 33 ID/OD 12/15 Eng. Pf = 2.75	Lh	0,1	34,0	119,8	103,3	12,1	76,9	23,3	37,7	1,5	2623

FATIGUE TESTS RESULTS

Fatigue tests experiments were performed at ITER relevant hydraulic conditions (i.e. 35 bar, 12 m/s, 140°C) with the following parameters:

- uniform heat flux profile;
- 110 mm length heated surface;
- pulse duration and dwell time : 10s ON / 10s OFF;
- ~20 MW/m² heat flux absorbed in the water.

Four mock-ups were fatigue tested : 2 mock-ups of 23 mm width (A23 and B23) an 2 others of 28 mm width (B28 and C28).

It was not possible to fatigue at 20 MW/m² a 33 mm width mock-up due to too high temperature reached during increase power (more than 2500°C for 17 MW/m²).

A view of the 4 mock-ups fatigue tested after 1000 cycles at 20 MW/m² is proposed figure 2.

Even if the screening cross checked with non destructive examination have shown that the bonding interfaces present some defects (specially on B28 with DTref > 15°C on SATIR and Tsurf on the edges up to more than 2400°C under 20 MW/m²), the cycling step was well sustained by the four mock-ups (see figure 2).

CRITICAL HEAT FLUX TESTING RESULTS

Following the usual procedure on FE200, 12 values of Critical Heat Flux (noted Max. AHF in table 1 for Maximum Absorbed Heat Flux) were measured on the 10 prototypes.

Results for the 23 mm width mock-ups:

The 2 CHF obtained with uniform incident heat flux confirm the previous results measured on a prototype tested in 1999 (PRODIV1), i.e. 22 MW/m² for representative ITER thermal hydraulics conditions (~12 m/s, 35 bar, 140°C). TONG75 modified correlation gives a good prediction of such a value (the error range being +/- 20 %). In case of peaked heat flux, a higher CHF of 35.4 MW/m² is found, giving a comfortable margin with regards to ITER nominal conditions.

Results for the 28 mm width mock-ups:

Three CHF were measured on the 28 mm width, 3 mm thickness mock-ups with some discrepancies : width effect is not evident, two values being higher than in 23 mm case (24.2 and 24.9 MW/m², see table 1), the third one being lower (19.9 MW/m²) but may be attributed to a bonding defect. Two CHF were measured on the 28 mm width, 8 mm thickness mock-ups. This mock-up was tested at moderate thermo hydraulic conditions because of the expected limitations on surface temperature : low velocities were chosen (5.1 and 3.3 m/s) and led to CHF as high as 19.3 and 17.9 MW/m² explained by a post-CHF regime when low velocities are used.

Results for the 33 mm width mock-ups:

Three CHF were measured on the 33 mm width, cooling tube ID/0D 10/12mm mock ups : 20 MW/m² was not systematically attained even at velocities as high as 12 m/s, moreover, surface temperature reach up to 2500°C at ICHF. One CHF of 23 MW/m² was measured on the 33 mm width, cooling tube ID/0D 12/15mm, such geometry appearing finally as performing as 23 mm width, ID/0D 10/12mm.
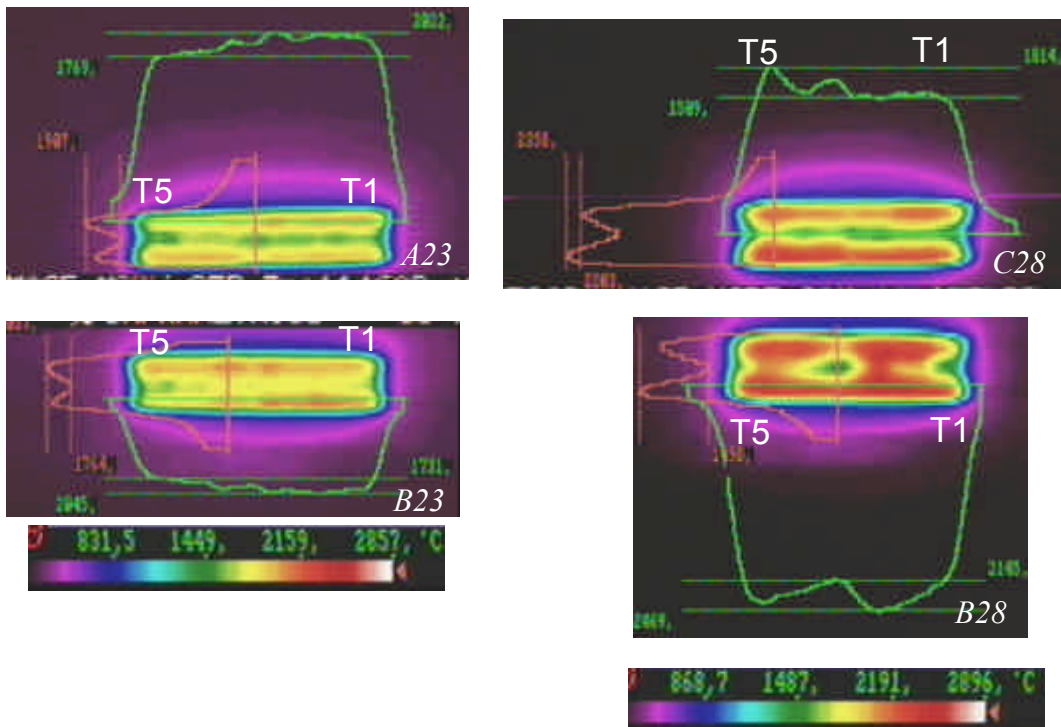
Figure 2 : The 4 fatigue tested mock-ups after 1000 cycles at 20 MW/m²

CONCLUSIONS

Ten CFC NB31 monoblock with 3 different widths (23, 28 an 33 mm) were fatigue tested and Critical Heat Flux (CHF) tested on the FE200 facility in the frame of this contract.

Both the 23 and 28 mm width mock-up meet the design requirements (1000 cycles at 20 MW/m² + CHF higher than 20 MW/m²).

As regards the 33 mm width monoblock, too high surface temperature did not allowed fatigue testing to be done. Moreover, it was found that it is necessary to increase the tube diameter from 10/12 mm to 12/15 mm ID/OD in order to obtain the same CHF performance than with the 23 mm width monoblock.

REPORTS AND PUBLICATIONS

[1] F.Escourbiac, «Spécifications techniques pour la maquette CHF-monobloc à tester au FE200 », CEA report CFP-NTT/2002-023, june 2002.

[2] F.Escourbiac, «Contract 99-501 : Critical heat flux testing of monoblock mock-ups- Final report», CEA report CFP-NTT/2002-035, Dec. 2002.

[3] I. Bobin Vastra "Mock-up CHF monoblocks : fatigue testing and critical heat fluxes on 10 CFC-NB31 elements", FRAMATOME report TFCW R 02. 884 A, Dec. 2002.

TASK LEADER

F. ESCOURBIAC

DSM/DRFC/SIPP
CEA Cadarache
13108 Saint Paul Lez Durance Cedex

Tél. : 33 4 42 25 44 00
Fax : 33 4 42 25 49 90

E-mail : frederic.escourbiac@cea.fr

**Task Title: CRITICAL HEAT FLUX TESTING OF HYPERVAPOTRONS
200 kW electron beam gun test**

INTRODUCTION

Heat fluxes (5-20 MW/m^2) to be removed by specific plasma facing components (PFC) in ITER are in the same range than observed in the klystron of electronic tubes. Fin enhancement cooling concepts with boiling/condensation effect, named vapotron® (1950) and then hypervapotron® (1973), were developed by Thomson CSF Company [1]. As far as ITER PFC are concerned, the hypervapotron® concept with flat tile armour is an interesting alternative to tubes with swirl insert armoured with monoblocks [2] because:

- bonding of flat tiles is easier;
- volume of armour material attached to the heat sink is lower and the concept is expected to be cheaper;
- the Critical Heat Flux (CHF) is higher for hypervapotron® than for swirl tubes for the same width of compared elements [3][4].

In addition of the possible use in the divertor vertical target, the hypervapotron® cooling is also envisaged in the divertor dome component.

Hence, it is necessary to measure and analyze CHF limit of different hypervapotron® (HV) metallic mock-ups in order to consolidate and enlarge the critical heat flux database on this type of geometry including cooling conditions foreseen for the dome.

2002 ACTIVITIES

TEST SECTIONS

Nine metallic prototypes with 3 different widths of 27; 40 and 50 mm were manufactured by CEA. To allow the repetition of CHF tests, samples are identical 3 by 3, respectively identified HV27-i, HV40-i and HV50-i; i being a number varying from 1 to 3. The cross section geometry is given figure 1: a slot of 1 mm is machined on the edges of the channel.

Practically, useful length of each component is 300 mm, overall length being 555 mm including inlet and outlet parts. Each prototype is made of Glidcop Al 25 (dispersion strengthened copper 0.25 % Al$_2$O$_3$ manufactured by SCM, USA). Although it is not relevant for ITER this material has a good behaviour at temperature higher than 600°C expected during CHF experiments and simulates well the thermal conductivity of CuCrZr alloy that would be used for ITER.

After milling of the grooves on the rectangular bars, rear plates were electron beam welded to close the channel (see figure 2). During final machining, inlet and outlet were turned to obtain a transition for circular tube connection.
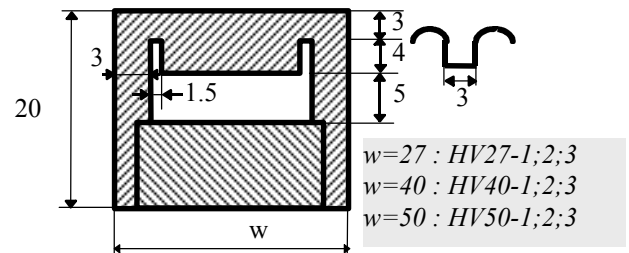
Figure 1 : Schematic drawing of tests samples
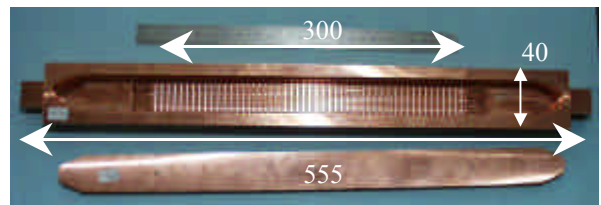
Figure 2 : Rear view of HV40-1 before EB welding

EXPERIMENTS AND TEST MATRIX

CHF experiments were performed using the European high heat flux facility FE200 [5][6]. Incident power on the heated mock-up was increased step by step for a set of parameters: heated length (100-200 mm), inlet water temperature (65-103°C), pressure (32-34 bar) and flow rate (0.3-1.1 kg/s) up to the detection of abnormal variation on surface temperature measured by infrared thermography and pyrometers and marking a burn-out. Maximum absorbed power at steady-state before this abnormal variation was computed and allowed the calculation of the so-called Incident Critical Heat Flux (ICHF), the radiative power being negligible.

Following this procedure, 54 values of ICHF were measured on the 9 prototypes, they were systematically detected at the outlet section where the subcooling is the lowest (cf. figure 3).

Several values of parameters were investigated during the testing campaign : flow rate (3 values between 2 and 6 m/s), incident heat flux profile (uniform 100 mm or peaked 200 mm length, see figure 4) and width of the prototypes (27, 40 and 50 mm). The inlet temperature was adjusted with pressure to tentatively obtain a constant outlet subcooling. Low axial velocities values were chosen for possible application in the ITER divertor dome cooling.
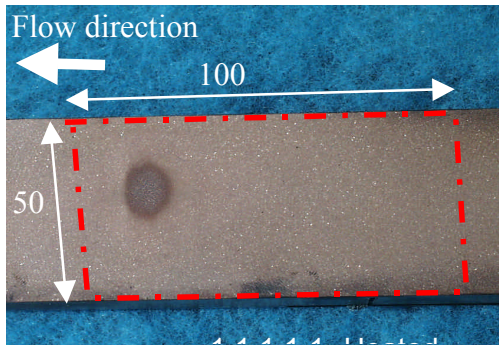
Figure 3 : Detection of burn-out
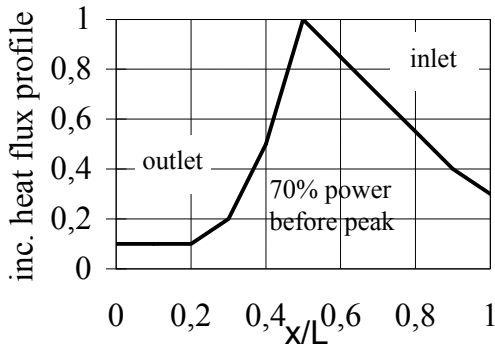
Figure 4 : FE200 peaked profile

Figure 5 : ICHF vs velocity
(32-34 bar, 113 –127°C subcooling)
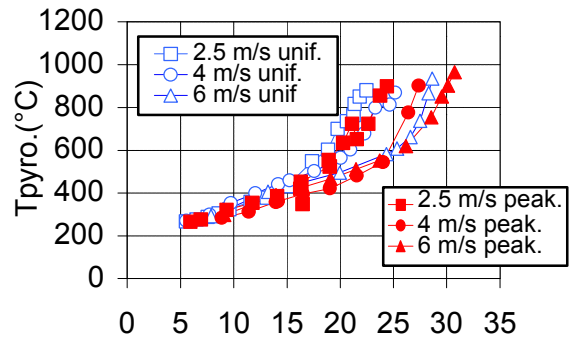
Figure 6 : Pyrometers temperature vs incident heat flux
in MW/m² (HV27-2)

Figure 7 : ICHF vs width (mm)

RESULTS AND DISCUSSION

ICHF values for the 9 mock-ups as a function of axial velocity, both for uniform and peaked heat flux are presented figure 5.

For the same set of parameters, each ICHF detection was repeated 3 times in order to increase the reliability of the measurements (however the accuracy of ICHF, calculated from calorimetry, is 8 %).

The data match the value obtained during 1996 testing campaign [3]. It is further confirmed that an incident uniform heat flux of 28 MW/m² can be reached without burn-out for a 27 mm width hypervapotron®, 5 m/s axial velocity and ~120°C subcooling, as considered for the ITER dome and possibly for the vertical targets.

An important result of the campaign is the negative effect of the width on the ICHF (figure 7): from 27 mm to 50 mm width, ICHF decreases more than 30 % in case of uniform profile and of 10-20% for peaked profile.

One can assume that water enters better the slots from the lateral 1.5 mm groove if the mock-up is narrow, this effect being less important with peaked heat flux.

The measured surface temperature during the tests correspond to the joint temperature of an armored flat tile component. This temperature at 20 MW/m² depends on the water velocity and on the shape of the flux, varying from 450°C to 700°C in case of 27 mm width hypervapotron (cf. figure 6), it may be the limitation of such a concept.

Pressure drop of the mock-ups were carefully measured after CHF experiments at ambient temperature in the range 0.1-5 bar, 0.1 – 1.5 kg/s with an accuracy of less than 3 % on the high velocity pressure drop test bed of CEA Cadarache. Small holes for pressure gauges connections were machined directly upon the fins avoiding inlet and outlet perturbations. Results are reported figure 8 as a function of velocity for each prototype and compared with Baxi's correlation for HV27 [7].

For a given velocity, pressure drop per unit length is increasing when the width of the mock-up decreases but still lower than for swirl tube, shown for comparison.

On the other hand, for given axial velocity, flow rate decreases when prototype width increases. Pumping power - defined as pressure drop times volumic flow rate - is a well adapted parameter for comparison between various tubes: it indicates the power needed to feed a tube with the required flow rate and pressure drop (Figure 9). The hypervapotron concept needs a lower pumping power than swirl tube. For example to remove a uniform heat flux of 25 MW/m², HV50, HV40 and HV27 requires respectively ~40, 100 and 150 W/m of pumping power whereas a 27 mm double swirl tube with two channels of 10 mm diameter needs 300 W/m [4].
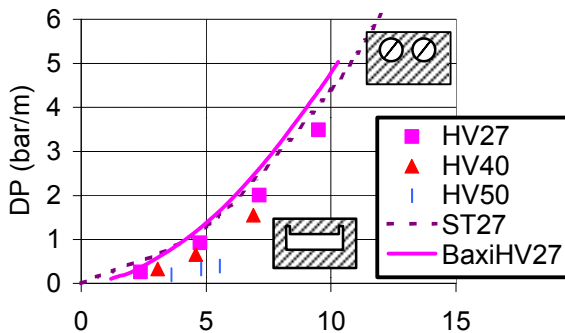
Figure 8 : Pressure drop vs flow rate
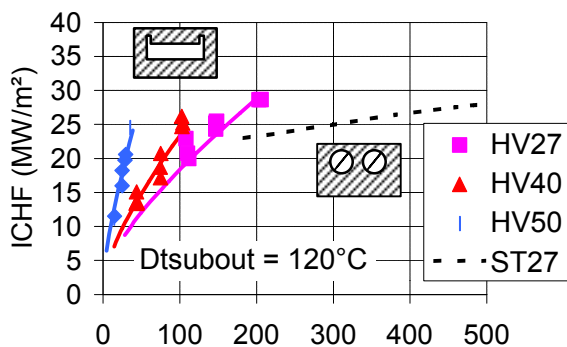
Figure 9 : ICHF vs pumping power

CONCLUSION

Nine metallic hypervapotron® tubes with 3 different widths were CHF tested. The 54 points of measurements obtained at 120°C constant subcooling have shown that for the 27 mm width, heat flux up to 25-30 MW/m² can be removed with an axial velocity as low as 4-6 m/s. However surface temperature at 20 MW/m² may be the limit for the hypervapotron® concept as far as flat tile armour is concerned. ICHF was also found depending on hypervapotron® width. These conclusions enlarge the previous data base, confirms the good performances of hypervapotron compared to swirl tube concept.

REFERENCES

[1] A. Beurthereut , Transfert de flux supérieur à 1kW/cm² par double changement de phase entre une paroi non isotherme et un liquide en convection forcée, presented at the 4th IHT conference, Versailles, Sept. 1970.

[2] J. Schlosser, F. Escourbiac, M. Merola, G. Vieider, Thermal hydraulic testing for ITER high heat flux components, Fusion Technology 1998, Proc. of the 20th SOFT , Marseille 1998, pp 137-140.

[3] I.Smid, J.Schlosser, J.Boscary, F.Escourbiac, G.Vieider, Comparison between various thermal hydraulic tube concepts for the ITER divertor, Fus. Tech. 1996, Proc. of the 19th SOFT, Lisbon 1996, pp 263-266.

[4] J. Schlosser, J; Boscary, F. Escourbiac, M. Merola, G. Vieider, Thermal hydraulic design of high heat flux elements for controlled fusion, 15th IUT NHTC , Turin 1997, pp 45-59.

[5] G.Mayaux, A Cardella, P. Chappuis, P; Deschamps, M. Febvre, J. Y. Journeaux, H. Viallet, 200 kW Electron gun facility for PFC's tests, Fus. Tech. 1992, Proc. of the 17th SOFT, Rome 1992, pp 317-321.

[6] M.Diotalevi, M.Febvre, Evolution of FRAMATOME and CEA HHF station for fusion experiments, Fus. Tech. 1996, Proc. of the 19th SOFT, Lisbon 1996, pp 491-494.

[7] C.Baxi, "Proposed design correlations for the hypervapotron", ITER/US/95/IV-DV-05, Section 1.3.5.

REPORTS AND PUBLICATIONS

[8] F.Escourbiac, "Spécifications techniques pour la maquette HV2002 à tester au FE200 », CEA report CFP/NTT/2002-007, April 2002.

[9] F.Escourbiac, "Contract 01-581 : Critical heat flux testing of hypervapotron - Final report , CEA Report CFP/NTT/2002-034, Dec. 2002

[10] F.Ecourbiac, J. Schlosser, M. Merola, I. Bobin Vastra, "Experimental optimisation of a hypervapotron® concept for ITER plasma facing components", Proc of the 22th SOFT, Helsinki 2002, to be published.

[11] I. Bobin Vastra "Mock-up HV2002 : 54 critical heat fluxes on Copper based Hypervapotron elements", FRAMATOME report TFCW R 02. 882 A, Nov. 2002.

TASK LEADER

F. ESCOURBIAC

DSM/DRFC/SIPP
CEA Cadarache
13108 Saint Paul Lez Durance Cedex

Tél. : 33 4 42 25 44 00
Fax : 33 4 42 25 49 90

E-mail : frederic.escourbiac@cea.fr

Not available on line

Not available on line

Task Title: **OPTIMISATION AND MANUFACTURE OF HHF COMPONENTS**
Study of flat tile cascade failure possibility for high heat flux components

INTRODUCTION

The object of this task is to evaluate the possibility of failure in cascade of flat tiles under convective heat flux with a glancing incidence.

Calculations and tests on the high heat flux (HHF) facility FE200 are planned.

Preliminary works in 1999 consisted in the definition of the geometry, the study of the feasibility of the tests by finite elements calculations and the definition of foreseen tests and mock-ups to be prepared.

In 2002 the mock-ups were delivered by Plansee: 2 of them armoured with NB31 CFC flat tiles and 2 of them with pure-W castellated flat tiles.

The tests were defined [1] and launched on the FE200. Only the mock-ups with CFC tiles were tested in 2002. The tests gave very good results with no evidence of cascade failure.

2002 ACTIVITIES

RECALL OF THE OBJECTIVES

The flat tile with hypervapotron (HV) cooling has the following advantages:

- It is cheaper than the corresponding monoblock geometry by about 25 % (excluding the armour cost).

- The armour cost is reduced by about 50 %.

- The width of the VT unit can be increased appreciably.

- The surface temperature is more uniform.

- It has a higher critical heat flux limit and a lower pumping power with respect to the "swirl tube" with a twisted tape having a twist ratio of 2.

- A curved component can be manufactured without adding significant manufacturing issues.

- The thickness of the cooling tubes is not intrinsically limited to 1 mm as for the monoblock geometry. It is worth noting that the cooling tubes represent the only boundary between the pressurised water coolant and the plasma vacuum chambers.

- It is a more mature technology and is already foreseen in existing tokamaks.

However the following issues needs to be investigated:

- It generates significantly higher cyclic thermal stresses than monoblock geometry; therefore the thermal fatigue lifetime is lower (19 MW/m^2 x 1000 cycles vs. 24 MW/m^2 x 1000 cycle for a flat tile and monoblock geometry, respectively). This is particularly important in the bottom part of the VT where the highest heat flux will occur.

- In the case of a convective heat flux, as for the lower part of the VT, one should also take into account that if one tile falls off, the adjacent tile receives an extremely high heat flux localised on its edge as a consequence of the glancing incidence. As a result a rapid temperature rise occurs in the armour - heat sink joint, which might seriously damage the joint. The heat flux to the coolant also increases significantly thus causing possible critical heat flux problems.

This last point is the objective of this task.

MOCK UPS DELIVERY

Four mock-ups were delivered by Plansee Company (figure 1). Two of them were made of NB31 CFC flat tiles bonded to a hypervapotron CuCrZr heat sink
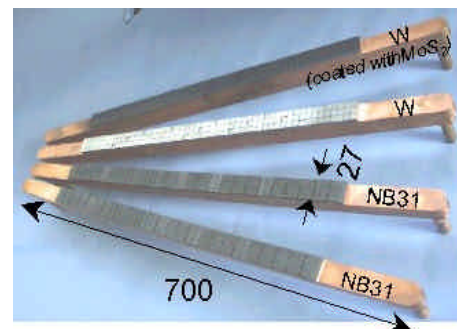
Figure 1 : The 4 mock-ups as delivered by Plansee

The amour is composed of 25 19.2x27 mm^2 tiles each of them being 6 mm thick except some tiles which are machined to 5 mm: tiles 6, 10, 13, 21 on the whole surface, 15 on the second half and tile 18 on the first half (figure 2).

SATIR TESTS AND FE200 SCREENING

SATIR tests did not give good results due to the lack of reference elements (figure 3). In these conditions it is very difficult to find correlations between SATIR testing and screening. The screening show rather good mock-ups with temperature at 6.4 MW/m^2 between 450 and 550 °C, the machined parts with lower temperature are well visible (figure 4).
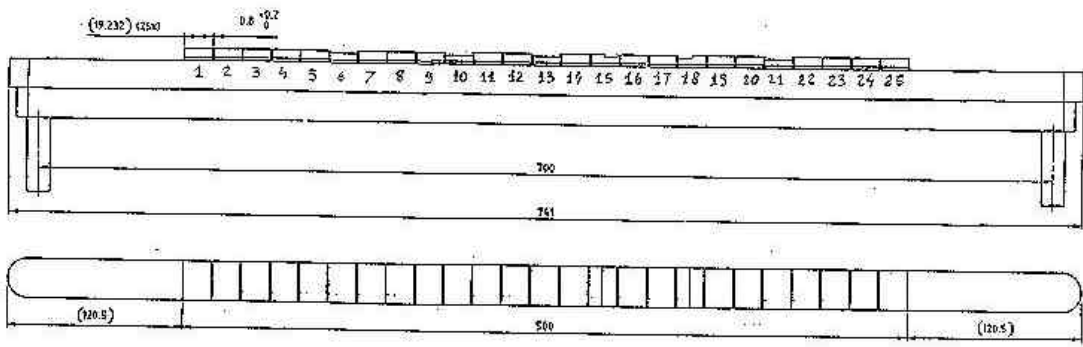
Figure 2 : Tile machining on the NB31 CFC mock-up
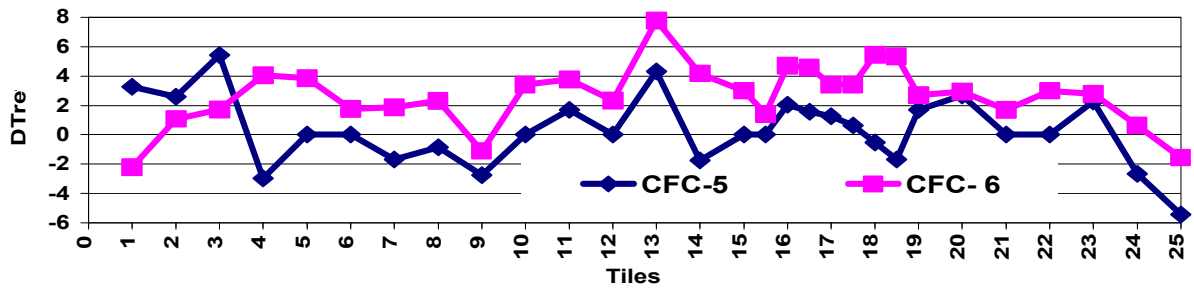
Figure 3 : Tile machining on the NB31 CFC mock-up
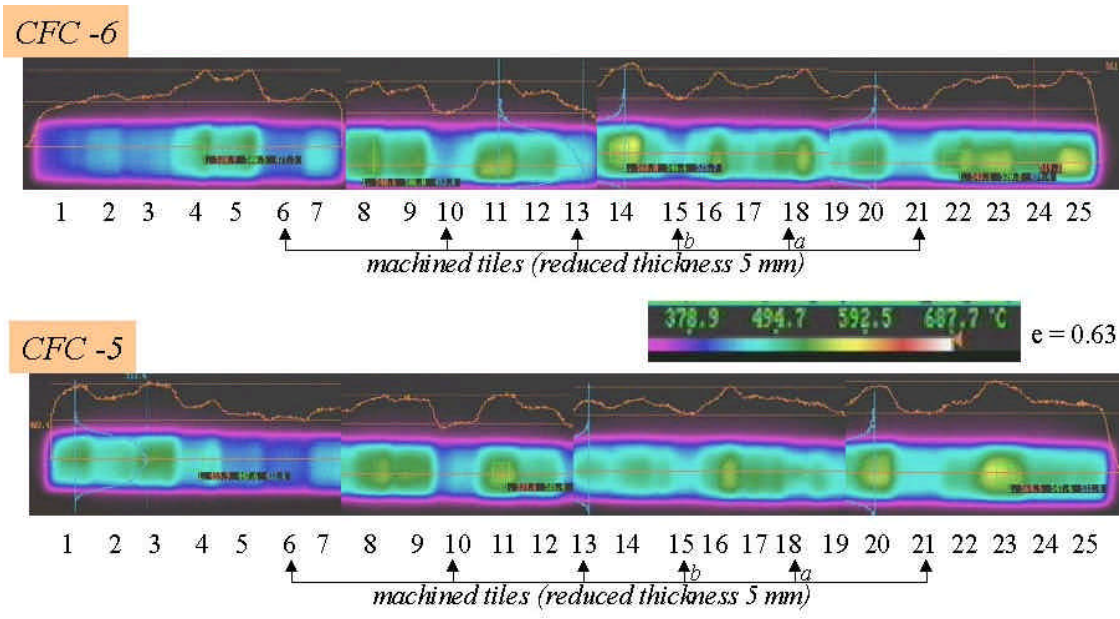
Figure 4 : Screening at 6.4 MW/m² showing well the machined parts
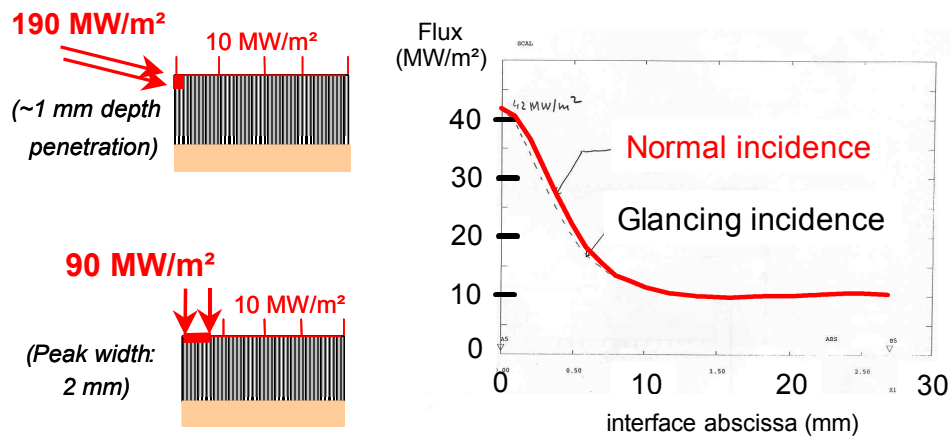
Figure 5 : Comparison of heat flux profile at the CFC-Cu interface

TESTS WITH NORMAL INCIDENCE

It was shown by calculation (figure 5) that it can be possible to have almost the same heat flux at the CFC-Cu interface with a normal incidence profile than with a glancing incidence of 3°. As normal incidence tests are routinely operated in the FE200 it was decided to perform first a normal incidence testing.

Only one mock-up (CFC-5) was tested on 2 zones (figure 6). The incidence was 95° in order to avoid CHF between the tiles.
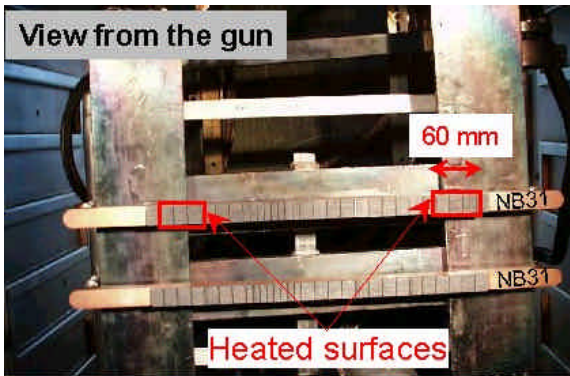
Figure 6 : View of the 2 NB31 CFC mock-ups in the vacuum chamber

The results obtained were rather in agreement with initial calculations with a surface temperature of 3015°C and a high erosion of the tile. Three hundred cycles were performed with the profile 10s on a zone and 10s on the other. The detail of the cycles is given table 1. The CFC/Cu bond was not damaged at the end of the tests but an important erosion of the CFC was observed (1.3 mm) (figure 7).

Table 1 : Cycling with normal incidence

Number of cycles	Power removed into the water (kW)	Local Max. IHF (MW/m²)
100	14	58
100	24	100
100	**28**	**117 (+30%/nominal)**

TESTS WITH GLANCING INCIDENCE

The principle layout of this test is given figure 8. The two mock-ups are positioned in the vacuum chamber so that an angle of about 3° with the beam is obtained (figure 9 and figure 10). The CCD camera was moved to the lateral window so that to obtain a front view of the mock-ups during the test (figure 10). A total of 500 cycles were performed at 190 MW/m^2 (equivalent to 10 MW/m^2 in normal incidence). The tile leading edges erosion occurred in 1 or 2 cycles only, and both IR and CCD views showed a stable situation for the rest of the cycles (figure 11).
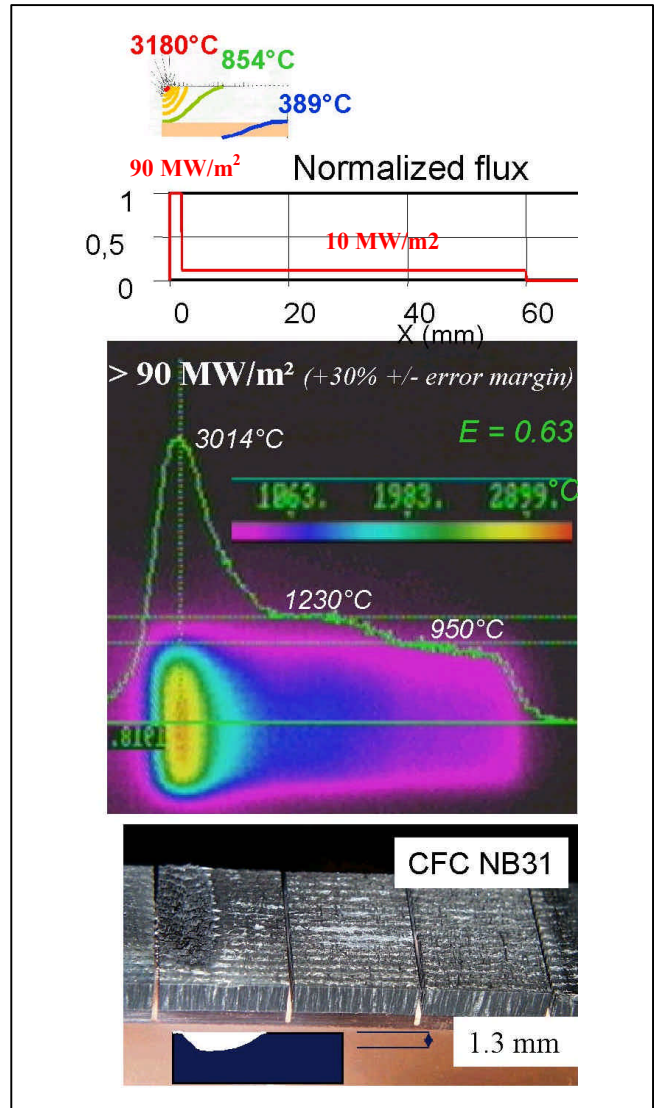
Figure 7 : Calculation, profile, IR view during the tests, and eroded surface at the end
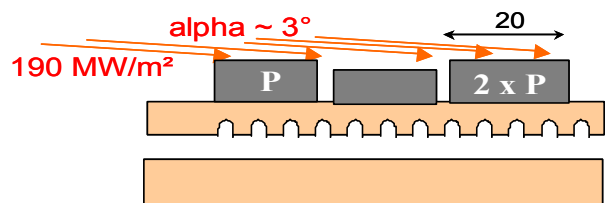
Figure 8 : Principle lay out of the glancing incidence test
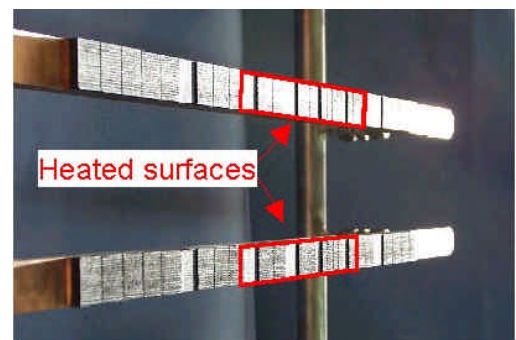
Figure 9 : The two mock-ups installed in the vacuum chamber for glancing incidence tests
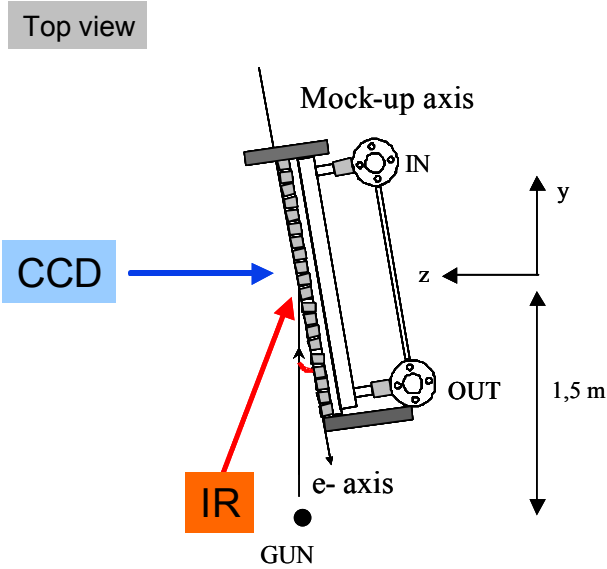
Figure 10 : Lay out of the glancing incidence test
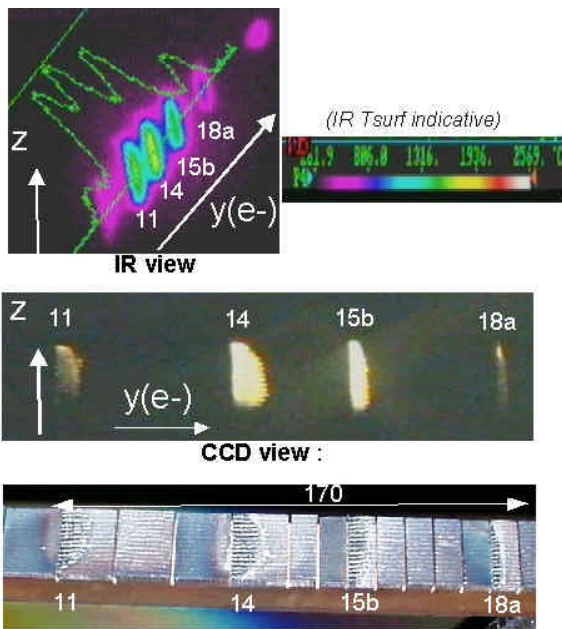
Figure 11 : IR view, CCD view and photograph of the mock-up at the end of the test

After the 500 cycles a shot of 1000 s was performed in order to check the stability of the IR image (table 2). After the test the mock-up showed an important shaping of the leading edges, but no damage of the CFC/Cu bond could be seen. The cascade failure did not occur.

Table 2 : Cycling with glancing incidence

Number of cycles	Power removed into the water (kW)	Local IHF (MW/m²) on the edge
500 (10s)	40 (+20% +/- error margin)	190 (+20% +/- error margin)
1 (1000s)	40	190

CONCLUSION

The expected phenomenon of cascade failure did not occur during the tests, showing that the hypervapotron cooling is probably more efficient than calculated. This concept of hypervapotron heat sink armoured with CFC flat tiles becomes then an attractive alternative design for the vertical targets of ITER.

The task will continue in 2003 with the tests on the Tungsten mock-ups.

REPORTS AND PUBLICATIONS

[1] F. Escourbiac, J. Schlosser, Spécifications techniques pour la maquette « Cascade failure » à tester au FE200, CFP/NTT-2002.031, 23/10/2002.

TASK LEADER

Jacques SCHLOSSER

DSM/DRFC/SIPP
CEA Cadarache
13108 Saint Paul Lez Durance Cedex

Tél. : 33 4 42 25 25 44
Fax : 33 4 42 25 49 90

E-mail : jacques.schlosser@cea.fr

Task Title: DEVELOPMENT AND TESTING OF TIME RESOLVED EROSION DETECTING TECHNIQUES

INTRODUCTION

Carbon based material is widely used as plasma facing component in present fusion device due to its good thermophysical properties. This is also the material selected for the ITER divertor. Nevertheless, physical and chemical sputtering yield of carbon are important and this lead to high erosion rate. As a consequence, the large carbon source reacts with the plasma and creates a very complex Plasma Wall Interaction physic. In particular, carbon redeposition may occur when carbon atoms or ion return to the wall. Because of the reactivity of carbon with hydrogen, carbon layers are built up with a large hydrogen isotope content. In the case of ITER, the tritium retention in these carbon redeposited layers may limit the operation for safety reason.

So far, only basic erosion and redeposition measurements have been undertaken in present tokamak and none of them can provide in situ a time resolved erosion/redeposition measurement.

In the framework of the CIEL program [1], it is planed to obtain in Tore Supra high performances long time discharges (up to 1000 s). For such a duration, erosion of plasma facing components may become very significant. Therefore, Tore Supra being the only tokamak where erosion/redeposition for a single shot is similar to that expected in ITER, in situ diagnostic should be developed and tested in order to demonstrate our capability to monitor the codeposition process in ITER.

PREVIOUS RESULTS

For a 1000 seconds discharge, the resulting gross erosion on the LPT in CIEL was estimated to be in the range of 10^{20}C per cm^2 or 10 µm. Previous measurements performed on actively cooled carbon limitor on inner wall [2] have shown that the net erosion rate can be reduced, due to local redeposition, by 2 orders of magnitude. As a consequence, the erosion and redeposition process to measure should be in the range from 0.1 to 10 µm for a single discharge. From bibliography analysis [3], Speckle interferometry has been retained as the most promising technique.

Preliminary experiments [4] showed the feasibility of such technique on a carbon fibre material and provided qualitative and quantitative information on surface displacement. It was also shown that 2 wavelengths are required for a tokamak application. By using a second laser, it is possible to measure the relative displacement and to perform a shape measurement of the object to analyse. According to the proposal made last year [3], 2-wavelength speckle interferometry has been investigated.

2002 ACTIVITIES

The main objectives of the work performed in 2002 was to define the specifications of the lasers (wavelength, linewidth, power, pulse duration, frequency…) required for the speckle interferometer. For that purpose, different lasers source have been tested. Experiments have been performed in CEA Saclay by using a continuous and accordable Dye laser pumped with an Argon laser. The argon laser has an output power of 10 W at 514 nm and the Dye laser about 400 mW at 570 nm.

The laser beam was transmitted to the speckle interferometer through a 50 m optical fibre. The coherence length of such a laser is very large (~ 300 m) due to the very small linewidth of this laser (Ring CR-699 from Coherent). Depending of the values of the wavelengths, the synthetic wavelength, $\Lambda = \dfrac{\lambda_1 \cdot \lambda_2}{|\lambda_1 - \lambda_2| \cdot \cos\theta}$ could be varied of several order of magnitude, in order to be adjusted to the range of the measurement to perform. Temporal Phase shifting technique with 4 phases has been used for each wavelength.

From the eight pictures acquired, we calculated two phase images (one for each wavelength). By differentiation of these two phase images, we obtain a 3D measurement of the object.

First experiments have been conducted on a 1 € coin, by using laser wavelength of 572,250 and 573,000 nm, resulting in a synthetic wavelength, Λ of 438 nm. The figure 1 shows the contour plot of a 3D view of 1€ coin as well as a line profile across the coin, showing a relief value in the range of 200 µm.

Nevertheless, the device is very sensitive to vibrations, which caused great difficulties to get correct measurements. Therefore, a pulsed laser with a short pulse length (few ns) is required in order to "freeze" the vibrations. Following these experiments, a Call for Tender has been launched for the procurement of a pulsed and accordable laser with a large coherence length.

The system which has been retained consists of a dye laser pumped by a pulsed Yag laser from Continuum. The lasers have been delivered at Cadarache in December. The installation in a clean room and commissioning are under progress.

In May, a paper has been presented at the PSI conference in Gifu, Japan and in November, an oral presentation has been done at a conference hold by the Societe Francaise d'Optique in Bordeaux
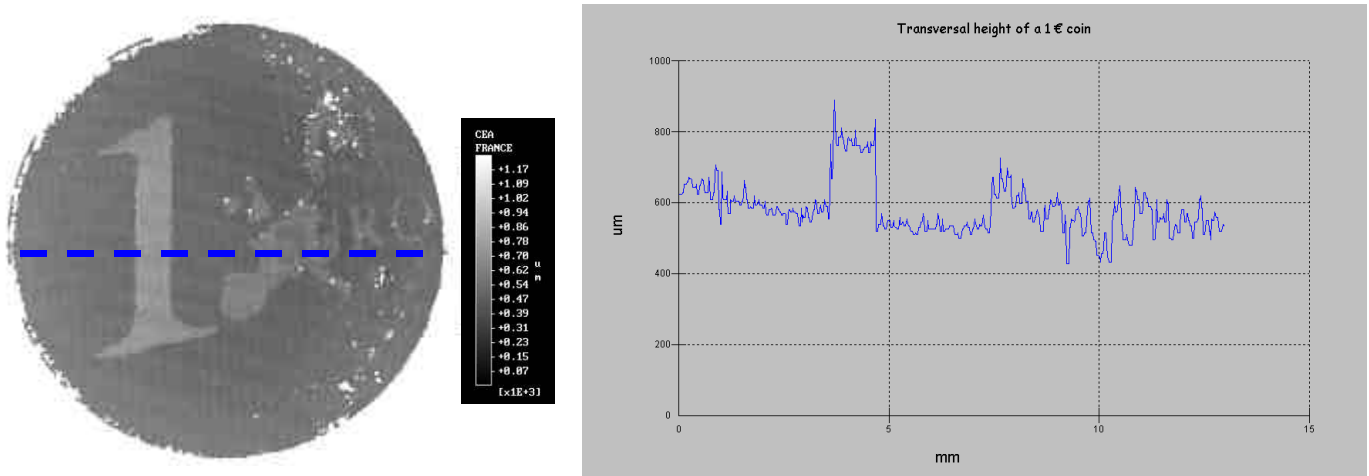
*Figure 1 : Contour plot of a 3D measurement of 1 €uro coin performed
with continuous dye laser and horizontal line profile across the coin*

CONCLUSIONS

Two-wavelength speckle interferometry measurements were conducted by using an argon and a dye laser. First experiments performed in CEA Saclay with a continuous laser using two wavelengths at 572.250 and 573.000 nm has provided 3D measurements in the range of 200 μm on a 1 € coin. This device was found to be very sensitive to vibrations. On the basis of these experiments, a new device based on pulsed and accordable laser was defined and specifications of the lasers required for a speckle interferometer were issued accordingly.

The lasers have been delivered at Cadarache, installation in a clean room and commissioning are under progress. Further experiments with 2-wavelength Speckle interferometry are planed in a CEA laboratory to validate the proposed design prior to a possible installation on Tore Supra. In particular we will investigate methods to increase the dynamic range and the resolution of the depth measurements and we will study the behaviour of the speckle interferometry measurements as function of the surface roughness of the material.

REFERENCES

[1]   P. Garin, Fusion Engineering and Design, vol. 49-50 (2000) 89-95.

[2]   E.Gauthier et al, J. Nucl. Mater., 220-222, (1995) 506-510.

[3]   G. Roupillard, CFP/NTT.2000.031, CEA Cadarache, 2000.

[4]   CEA rapport DSM/DRFC T438-01 2000.

[5]   CEA rapport DSM/DRFC T438-01 2001.

REPORTS AND PUBLICATIONS

Speckle Interferometry diagnostic for erosion/redeposition measurements in tokamaks - 15th Int. Conf. on Plasma Surface Interaction in Controlled Fusion Devices - Gifu (Japan), 27/05/02 - 31/05/02 - E. Gauthier, G. Roupillard.

Mesure in situ de l'érosion des composants internes dans Tore Supra par interférométrie Speckle - G. Roupillard, E. Gauthier, A. Petit, D. L'hermite, 3ème Colloque Francophone : Méthodes et Techniques Optiques pour l'Industrie - Saint Aubin du Médoc (France), 18/11/02 - 22/11/02.

Tests de lasers accordables pour le montage d'interférométrie speckle à deux longueurs d'onde 1. test d'un laser à colorant - G. Roupillard, E. Gauthier, CFP/CRM-2002.005.

Appel d'offre pour l'achat de lasers - E. Gauthier, CFP/CCH-2002.006.

Interim Report TW0-T438-01 Speckle Interferometry - E. Gauthier, G. Roupillard, CFP/NTT-2002.028.

TASK LEADER

Eric GAUTHIER

DSM/DRFC/SIPP/ICI
CEA Cadarache
13108 Saint Paul Lez Durance Cedex

Tél. : 33 4 42 25 42 04
Fax : 33 4 42 25 49 90

E-mail : gauthier@drfc.cad.cea.fr

Task Title: NEUTRON EFFECTS ON DIMENSIONAL STABILITY AND THERMAL PROPERTIES OF CFCs

INTRODUCTION

Carbon Fiber Composites (CFCs) are considered as an attractive choice for high heat flux components in existing and forthcoming tokamaks such as ITER. Two CFCs are particularly interesting for fusion devices: NB31 from SEP which is a 3D CFC constituted by a NOVOLTEX preform, with P55 ex-pitch fibers in the high thermal conductivity direction and NS31 which is a Si doped 3D N31 CFC [1].

The aim of this report is to give specific heat capacity and thermal conductivity changes of NB31 CFC and NS31 CFC irradiated at low temperature (250°C/260°C) in the PARIDE (**Pl**Asma facing mate**RI**als for ITER and **DE**MO) irradiations. These irradiations take place in the High Flux Reactor for two neutron damage levels: 0.24 dpa.g (PARIDE 3) and 0.83 dpa.g (PARIDE 4). Moreover the γ activity of the different radionucleides contained in these two CFCs have been measured.

Initially the thermal conductivity of these two irradiated CFCs had to be measured ; unfortunately, the γ dose rate of irradiated NS31 thermal diffusivity samples was too high, and their thermal conductivity could not be measured in our glove-box facility. So, only the NB31 thermal conductivity was measured.

A second irradiation with the same CFCs was carried out in SINTEZ reactor (Russia) at 100°C and at low neutron damage levels (0.001 dpa, 0.003 dpa, 0.01 dpa, 0.03 dpa, 0.1 dpa). But irradiated samples are not yet available.

2002 ACTIVITIES

POST-IRRADIATION RESULTS OF HIGH THERMAL CONDUCTIVITIES CFCs [2]

The density measurements of the NB31 samples were carried out in the ForschungsZentrum Juelich (FZJ, Germany). The NB31 density changes were 0.05 % in the PARIDE 3 irradiation, and 0.52 % in the PARIDE 4 irradiation. The density changes in both irradiations are negligible.

NB31 heat capacities after irradiation in PARIDE 3 and PARIDE 4 were measured with a SETARAM DSC 111G calorimeter. The results show that there is no change in NB31 heat capacity (according to the fact that uncertainty on the Cp measurement is ± 2.5 %) whatever are the irradiation conditions 260°C/0.24 dpa.g or 250°C/ 0.83 dpa.g.

After irradiation at 250°C/0.83 dpa.g, the NS31 heat capacity increases of 3-4% at 25°C and 50°C; for higher measurement temperatures, there is no change in NS31 heat capacity.

NB31 thermal conductivities (K_i) were calculated using results of average irradiated thermal diffusivities (D_{irr}) measured by laser flash method, average irradiated heat capacities (Cp_{irr}) and average densities of irradiated materials (ρ_{irr}). Thermal expansion coefficients of the unirradiated materials were used for ρ_{irr} calculations at high temperature :

$$\rho_{irr}(T°C) = \frac{\rho_{irr}(25°C)}{1+[(\alpha(x)+\alpha(y)+\alpha(z))\times(T°C-25°C)]}$$

with : $\alpha(x)$: average thermal expansion coefficient (20°C-800°C) of the unirradiated material in the x direction

$\alpha(y)$: average thermal expansion coefficient (20°C-800°C) of the unirradiated material in the y direction

$\alpha(z)$: average thermal expansion coefficient (20°C-800°C) of the unirradiated material in the z direction.

The irradiated NB31 thermal conductivity is given by the relation:

$$K_i = D_{irr} \times Cp_{irr} \times r_{irr}$$

The NB31 thermal conductivity results in the high thermal conductivity direction show a large decrease after irradiation in PARIDE 3 and PARIDE 4 (table 1).

Table 1

THERMAL CONDUCTIVITY OF NB31 IN X DIRECTION					
	Unirradiated	PARIDE 3 (260°C/ 0.24 dpa.g)		PARIDE 4 (250°C/ 0.83 dpa.g)	
Measurement temperature (°C)	K_0 (W.m^{-1}.K^{-1})	K_i (W.m^{-1}.K^{-1})	K_i / K_0	K_i (W.m^{-1}.K^{-1})	K_i / K_0
25	352.3	56.3	0.160	35.7	0.101
50	337.6	58.0	0.172	36.9	0.109
100	325.0	61.4	0.189	39.5	0.122
150	313.9	64.2	0.204	41.4	0.132
200	300.0	66.2	0.221	43.0	0.143
250	284.4	67.6	0.238	44.1	0.155

Moreover, we noticed that before irradiation, the NB31 thermal conductivity at 250°C was 3.1 times higher in the X direction than in the Z direction $((K_{0X}/K_{0Z})_{250°C} = 3.1)$. After irradiation at 260°C/0.24 dpa.g, this ratio $((K_{iX}/K_{iZ})_{250°C})$ decreases to 2.7; and after irradiation at 250°C/0.83 dpa.g, to 2.6.

This means, that the thermal conductivity in the X direction (high thermal conductivity direction) degrades a little more under irradiation than in the Z direction (low thermal conductivity direction).

In PARIDE 3 and PARIDE 4 experiments, irradiation temperatures are the same; even though the damage is 3.5 times higher in PARIDE 4 than in PARIDE 3. So, it is interesting to compare the neutron damage effect on the normalized thermal conductivity (K_i/K_0) in the three directions (table 2). When the neutron damage increases by a factor 3.5, the NB31 normalized thermal conductivity at 250°C decreases of 35 % in the X direction, 39 % in the Y direction and 31 % in the Z direction.

Table 2

	$(K_i/K_0)_{250°C}$ X direction	$(K_i/K_0)_{250°C}$ Y direction	$(K_i/K_0)_{250°C}$ Z direction
PARIDE 3 260°C / 0.24 dpa.g	0.238	0.289	0.269
PARIDE 4 250°C / 0.83 dpa.g	0.155	0.177	0.186

In previous works, we have shown that A05 CFC normalized thermal conductivity at 400°C and at 600°C is a logarithmic function of neutron damage, in a wide range of neutron damage (from 9.10^{-4} to 1.8 dpa.g) [3].

In previous works, we have shown that the normalized thermal conductivity at the irradiation temperature $((K_i/K_0)_{Tirr})$ of all investigated CFCs increases with increasing irradiation temperature between 400°C and 1500°C [4] (table 3).The NB31 normalized thermal conductivitiy $(K_i/K_0)_{250°C}$ is 0.16, after irradiation at 250°C/ 0.83dpa.g (almost 1 dpa.g). So it is clear that a low irradiation temperature avoids the annealing of the defects created by the neutron irradiation, therefore the propagation of the phonons along the graphitic planes is slowed down inducing a decrease of the thermal conductivity.

Table 3

Irradiation temperature (°C)	High K_0 CFCs ($K_0 > 300$ W.m^{-1}. K^{-1} at 25°C) $(K_i/K_0)_{Tirr}$ at 1 dpa.g	Low K_0 CFCs ($K_0 > 100$ W.m^{-1}. K^{-1} at 25°C) $(K_i/K_0)_{Tirr}$ at 1 dpa.g
400	0.30 - 0.35	0.30 - 0.35
600	0.55 - 0.60	0.60 - 0.65
800	0.75 - 0.80	0.85 - 0.90
1000	0.80 - 0.85	0.95 – 1
1500	1	1

γ spectrometry measurements were carried out in order to get an estimated value of the samples activity. The total average specific activities are:

- NB31 irradiated at 260°C/0.24 dpa.g : 4300 Bq/g (december 2002).

- NB31 irradiated at 250°C/0.83 dpa.g : 11400 Bq/g (december 2002).

- NS31 irradiated at 250°C/0.83 dpa.g : 280 kBq/g (december 2002).

The distribution of the total activity according to the main different radio-isotopes shows that the γ activity is mainly due to ^{60}Co.

CONCLUSION

The main conclusions which can be drawn are:

- The thermal conductivity changes are mainly determined by the thermal diffusivity changes. There is no density and heat capacity changes after irradiation.

- The thermal conductivity in the high thermal conductivity direction (X direction) degrades a little more under neutron irradiation than in the two others directions (Y and Z direction).

- At low irradiation temperature (250°C/260°C), for a neutron damage increase of 3.5, the ratio $(K_i/K_0)_{250°C}$ decreases of 31-39% according to the different directions.

- For high thermal conductivity CFCs, irradiadiated at 250°C/0.83 dpa.g, the ratio $(K_i/K_0)_{Tirr}$ is as low as 0.16. So it is obvious that the normalized thermal conductivity decreases with decreasing irradiation temperature.

- The NB31 and NS31 γ activities after irradiation at 250°C/0.83 dpa.g are 11.4 kBq/g and 280 kBq/g respectively. In both cases, the γ activity is mainly due to ^{60}Co.

REPORTS AND PUBLICATIONS

---

[1] Simulation experimental investigation of plasma off-normal events on advanced silicon doped CFC-NS31. J.P. BONAL, C.H. WU, D. GOSSET. Journal of Nuclear Materials 307-311 (2002) p. 100-105.

[2] Therrnal properties changes of carbon fiber composites irradiated at low temperature. PARIDE 3/4 experiment. J.P. BONAL. Rapport DMN SEMI/LM2E/RT/03-009/A.

[3]   Neutron induced thermal properties changes in carbon fiber composites irradiated from 600 to 1000°C.
J.P. BONAL, C.H. WU.
Journal of Nuclear Materials 230 (1996) 271-279.

[4]   Overview of EU CFCs development for plasma facing materials.
C.H. WU, C. ALESSANDRINI, J.P. BONAL, H. GROTE, R. MOORMANN, M. RODIG, J. ROTH, H. WERLE, G. VIEIDER.
Journal of Nuclear Materials 258-263 (1998) 833-838.

TASK LEADER

Jean-Pierre BONAL

DEN/DMN/SEMI/LM2E
CEA Saclay
91191 Gif-sur-Yvette Cedex

Tél. : 33 1 69 08 50 58
Fax : 33 1 69 08 90 82

E-mail : jean-pierre.bonal@cea.fr

JET-EP-Div

Task Title: JET EP DIVERTOR PROJECT

INTRODUCTION

The purpose of the enhancement was to consolidate the preparation of ITER operating scenarios, in particular with regard to ELMy H-mode operation in ITER-like configurations close to the operational boundaries and to support key ITER design choices which are still to be made. The project was developed since 2000 with an aim at producing the final specifications of all components ready for tendering in year 2002 in order to manufacture the divertor in 2003 and install the divertor during the 2004 shutdown. Because of financial restrictions, it was decided to stop the project at completion of the detail engineering phase.

2002 ACTIVITIES

The scope of work in 2002 was to finalize the project in a state which could be continued in the future if required.

DESIGN FINALIZATION

After the tile shape optimization for the 18 reference equilibrias, and the validation of the shadowed area (see figure 1), a new set of priority scenarios was established and detail thermal calculations were performed to asses the power handling capacity of the divertor

*Table 1 : Maximum pulse length for the high priority
scenario with 40 MW of injected power*

Config	Max average flux	Critical time
3.5MA_hd (workhorse high δ)	8.4 MW/m²	**10.1 s**
4MA_hd2 (higher Ip high δ)	8.12 MW/m²	**10.8 s**
2p5MA_hdhb (advanced scenario)	5.9 MW/m²	**19.9 s**
4MA_OS_swp15 (optimised shear)	8.18 MW/m²	**10.0 s**

The different operator interfaces were validated with the JET operator and a proposal for the remote handling installation was described.

The full set of the divertor components detail drawings of were achieved in April 2002.

The available diagnostic drawings were also included and space envelops were kept for the remaining ones (figure 2).
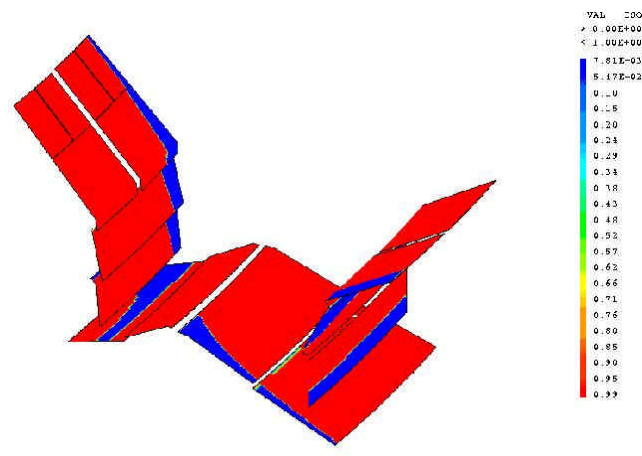
*Figure 1 : HP Divertor shadowed area
for HD2 equilibria*
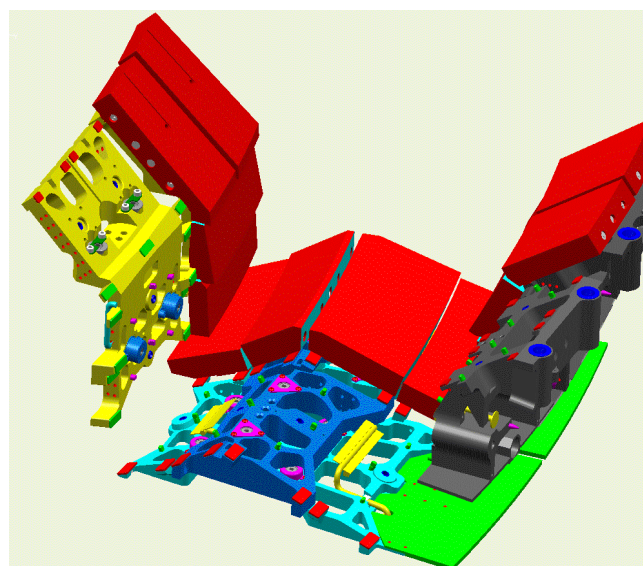
Figure 2 : HP divertor model

DELIVERABLES

The technical draft specifications for the carriers manufacturing and the tiles machining were delivered to the CSU JET.

The final report on the CEA activity, taking in account the reporting of 62 documents (references), was delivered in July 2002.

REPORTS AND PUBLICATIONS

[1] THE DESIGN OF A NEW JET DIVERTOR FOR HIGH TRIANGULARITY AND HIGH CURRENT SCENARIOS, Ph. Chappuis, C. Damiani, C. Guerin, F. Hurd, A. Loarte, P. Lomas, A. Lorenz, J. Paméla, A. Peacock, C. Portafaix, J. Rapp, V. Riccardo, F. Rimini, G. Saibene, JF Salavy, Y. Sauce, R. Sartori, E. Solano, E. Thomas, P. Thomas, E. Tsitrone, MP. Valeta ; 22nd SOFT, Helsinki 2002.

[2] DESIGN OF A NEW DIVERTOR FOR JET; Ph. Chappuis, C. Portafaix, F. Rimini, P. Thomas, E. Tsitrone, JF Salavy, MP Valeta, D. Campbell, F. Hurd, A. Loarte, M. Pick, A. Peacock, G. Saibene, R. Sartori, C. Damiani, J. Paméla, E. Solano, P. Lomas, V. Riccardo, IAEA TCM on Divertor Concepts, Aix en Provence 2001.

TASK LEADER

Philippe CHAPPUIS

DRFC/SIPP
CEA Cadarache
13108 Saint Paul Lez Durance Cedex

Tél. : 33 4 42 25 46 62
Fax : 33 4 42 25 49 90

E-mail : philippe.chappuis@cea.fr

Task Title: INTERNAL PFC COMPONENTS BEHAVIOUR AND MODELLING

INTRODUCTION

The knowledge of power and energy flux impinging on the divertor during Edge Localised Modes (ELMs) is a crucial issue for ITER. In JET, during experimental campaigns, the temperature is measured with an infrared camera and heat flux is deduced from code computation. During transient high heat loads the power calculated using standard material properties is over-estimated [1]. Indeed, the presence of a thin surface layer of codeposited material with low thermal conductivity induces a higher surface temperature for a given flux. In order to improve power estimation and provide tools for better power/energy measurements in tokamaks, model validations and experiments on divertor tiles are carried out using Castem code [2] and JET Neutral Beam test bed facility.

2002 ACTIVITIES

The scope of the work in 2002 was to define the tests to be performed, to prepare and install the required diagnostics, to specify the material properties for the bulk and the coated layer and implement them in the code. A second stage consisted in performing the tests and the modelling and comparing the results.

SETTING-UP THE TESTS

Tile 4 and tile 7 from the Mark IIa divertor have been selected because they were exposed to plasmas in JET during 1995-1996 campaign and surface analysis have shown codeposited layers [3]. Although the tiles were not Tritium contaminated, they were beryllium contaminated; machining of both tiles and thermocouples installation has been successfully achieved at JET Be workshop. A fast infrared camera was mounted on the test bed facility with optical fibre connection to the NB control room and successfully commissioned prior the experiments scheduled in July.

Unfortunately, the tests were postponed for several months due to three different water leaks in the NB test facility (the last one due to a bellow breakage induced one meter deep water in the tank). During the commissioning of the Be rig, few days before a second attempt in October, another water leak occurred again on a below, wasting any chance to perform the experimental tests in 2002.

MODELLING

A detailed 3-D model with true geometry of tiles with dumbbell, was developed using the CAST3M code (finite element code developed at CEA) to calculate the surface and in-depth temperature distribution on the divertor tiles.

The following heat loads have been considered for the experiments and the simulations:

- flux 100 MW.m^{-2}; 10 ms on, 10 ms off, 5 cycles,
- flux 50 MW.m^{-2}; 17 ms on, 43 ms off, 10 cycles,
- flux 5 MW.m^{-2}; 2 s on, 4 s off, 3 cycles.

Different material configurations have been calculated taking into account various thermal properties of the codeposited layers. Previous experiments [4] have showed that the bulk material properties may differ from the supplier specifications.

Therefore, various thermal conductivity values have been introduced in the code for both the bulk material and the coated layer (table 1).

Table 1 : Combination of bulk
and coating thermal properties used in the code.

	Bulk Thermal Conductivity K (% K_{ref} of CFC Dunlop)	Coating Thermal Conductivity K Thickness 40 μm (% K_{ref} of CFC Dunlop)	Heat exchange coefficient $H = \dfrac{\phi}{\Delta T}$
Cas0	100 %	No coating	
Cas1	100 %	10 %	
Cas2	70 %	10 %	
Cas3	50 %	10 %	
Cas4	30 %	10 %	
Cas5	70 %	30 %	
Cas6	70 %	50 %	
Cas7	70 %	30 %	$\Delta T = 50°C$
Cas8	70 %	30 %	$\Delta T = 250°C$
Cas9	70 %	30 %	$\Delta T = 500°C$

Part of the modelling was performed in CEA Saclay (see figure 1b) using a non uniform power profile as provided by the NB test bed (see figure 1a), while another part was done in CEA Cadarache using more material configurations with an uniform heat flux.

We consider the maximum surface temperature in the first case and the surface temperature at the thermocouple position in the second case, which allows a comparison of the data.

For a high heat flux of 50 MW.m^{-2}, the layer effect can clearly be seen on the surface temperature (see figure 2) while at a low heat flux of 5 MW.m^{-2}, the presence of the layer has no effect and only the bulk properties controls the surface temperature (see figure 3). These modelling results will have to be compared with the experimental results, when available.
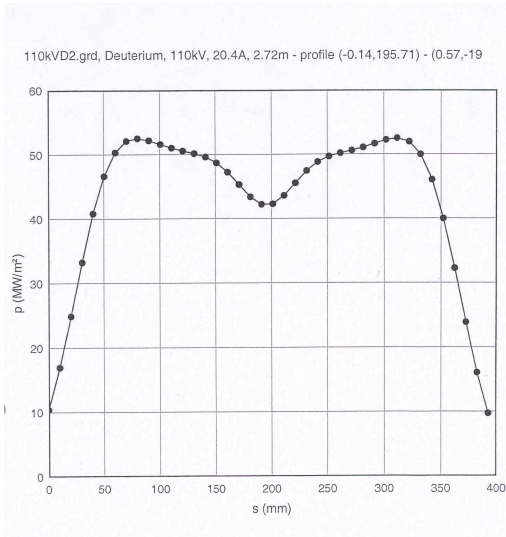
Figure 1a : Power density profile
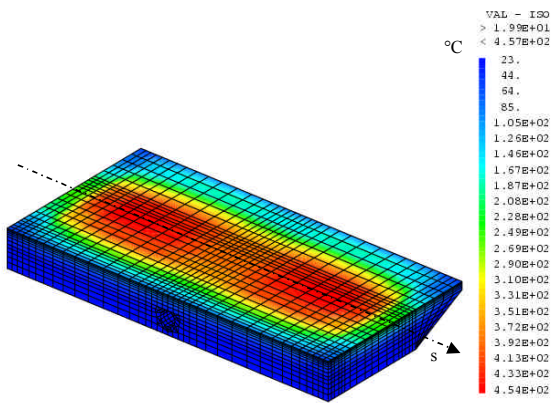
*Figure 1b : 100 MW/m² -
Temperature field at 0.260 second (without surface layer)*
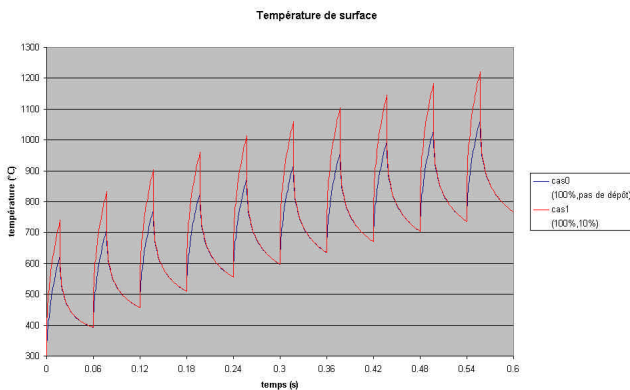
*Figure 2 : Surface temperature evolution at 50 MW/m²
with a surface layer (red) and without (blue)*
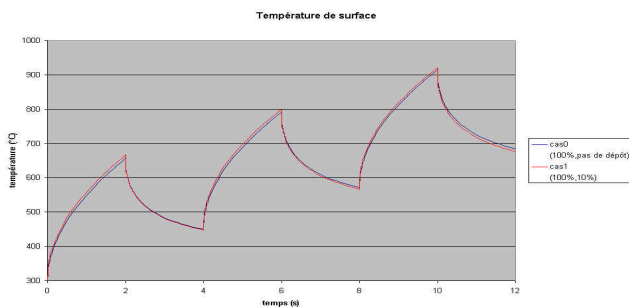
*Figure 3 : Surface temperature evolution at 5 MW/m²
with a surface layer (red) and without (blue)*

CONCLUSIONS

Modelling using Castem code with various material properties and different heat load conditions have been performed. Power deposition experiments at JET have been delayed due to several water leaks on the NB test Facility. Experiments are planned to be done in 2003 and results will be compared with modelling data in order to provide tools for better analysis of transient heat load during ELMS.

REFERENCES

[1] E.Gauthier et al, Proc. 24th EPS Conference, Berchtesgaden, (1997).

[2] P. Verpaux, A. Millard, A. Hoffman, L. Ebersolt, CASTEM 2000: A modern approach of computerized structural analysis. Proc. Recent Advances in Design Procedures for High Temperature Plant, Rislay, 1988.

[3] J.P. Coad et al, J. Nucl. Mater, 290-293 (2001) 224-230.

[4] S.Clement, A.Chankin, A.Ciric, J.P.Coad, J.Falter, E.Gauthier, J.Lingertat, S.Puppin, J. Nucl. Mater, 266-269 (1999) 285-290.

REPORTS AND PUBLICATIONS

Minutes of meeting on 13th February 2002 on task FT 3.1. CFP/CRR-2002.002 - E. Gauthier.

Simulation du comportement thermique d'une tuile du divertor MKIIA du JET. CFP/NTT-2002.027 - E. Gauthier, J. Matheus, M. Missirlian.

TASK LEADER

Eric GAUTHIER

DSM/DRFC/SIPP/ICI
CEA Cadarache
13108 Saint Paul Lez Durance Cedex

Tél. : 33 4 42 25 42 04
Fax : 33 4 42 25 49 90

E-mail : gauthier@drfc.cad.cea.fr

Task Title: THERMO-MECHANICAL MODELS (TMM)

INTRODUCTION

The general objective of this task is:

- to propose criterions and models which could be used in the operating conditions of high heat flux components in order to establish for each proposal its potential in terms of performances and lifetime,

- to perform studies, analysis and assessments related to thermo-mechanics for the plasma-facing component protection system (tiles, attachments) of present day tokamak.

2002 ACTIVITIES

RULES FOR DESIGN, FABRICATION AND INSPECTIONS

Although Fusion reactor blankets and high heat flux components are intended, in long-term, to operate under steady-state conditions, rupture conditions could be reached under series of thermal shocks occurring during the reactor lifetime. Impact on crack initiation and fatigue phenomena has to be clearly understood and interpretation and prediction rules have to be qualified on specific and relevant blanket loading conditions.

The knowledge of crack initiation from an initial defect (manufacturing or potential defect) can be today predicted by the σ_d rule, successfully developed and implemented by CEA over the past years and recently integrated in the French RCC-MR design code.

This action consists in the design of an experimental set-up that allows realising experiments of thermal fatigue for future validation of the σ_d criterion (crack initiation) for Eurofer-type 9Cr steel under blanket relevant thermal conditions.

Design of a thermal fatigue test:

Thermal fatigue tests with RAFM steel (Eurofer) or equivalent 9%Cr material are necessary to validate the criterion for Fusion applications (pure thermal loading conditions) but such tests were not found in the literature. So, the first stage of this action has consisted in the design of the experimental set-up up that allows realising experiments of thermal fatigue. The CEA technical note DM2S/SEMT/LISN/RT/02-009/A « *Progress in the design and construction of a thermal fatigue experimental set-up* » presents the principle of these thermal fatigue tests carried out on a pipe.

Realisation of thermal fatigue test and validation of sigma-d criterion:

This part concerns the feasibility of the test on a 316L specimen as reported in the CEA technical note DM2S/SEMT/LISN/RT/02-031/A "*Feasibility of a crack initiation test under thermal fatigue conditions*". A thermal fatigue test has been carried out on a 316L specimen and showed the performance of the experimental set up for fatigue crack initiation under thermal loading. A 3D finite element model has been introduced to estimate the number of cycles to crack initiation and then the test duration.

TILES INTEGRITY

Failure criteria for CFC materials can be used to evaluate the integrity of tiles used as plasma facing components under thermal and mechanical loads and to test the different designs.

The CEA technical note DM2S/SEMT/LM2S/RT/02-011/A "*Failure criteria for carbon fibber reinforced carbon composite (CFC)*" presents a preliminary study on the choice of a tile integrity criterion for carbon fibres reinforced carbon composites (CFC's): this criterion could be used in the operating conditions as parameters in order to establish for each proposal its potential in terms of performances and lifetime. A wide range of CFC materials can be considered for plasma facing components. The mechanical properties (which depend on raw materials, process and structure) are specific to each composite and may differ highly from a composite to another. The study indicates that the maximum stress theory or the Tsai-Wu criterion can be used for CFC.

COMPONENTS ANALYSIS

This activity was mainly focused on divertors and included thermo-mechanical linear analyses performed with CASTEM2000 finite element code developed in CEA associated with the retained criterion for tiles integrity.

Following a previous work performed in 2001, the mechanical integrity of plasma facing CFC tile was evaluated using a Tsai-Wu criterion and reported in the CEA technical note DM2S/SEMT/LM2S/RT/02-033/A "*Evaluation of CFC tile integrity using CAST3M and a Tsai-Wu criterion*".

Only elastic behaviour was taken into account resulting in an over-estimation of the Tsai-Wu strength function: calculations could be improved by modelling the non-linear behaviour of CFC composite. Moreover, the parameters of the strength function should be modified to take into account the secondary nature of the thermal loading which is less damageable than purely mechanical one.

SETTING ANALYSIS

In order to improve models used to calculate the thermo-mechanical behaviour of the plasma facing CFC tiles, the heat transfer coefficient between the tile and the dumbbell was taken into account. Realistic modelling of contact between the tile and the dumbbell was performed taking into account thermal conductance depending on contact pressure.

In the CEA report DM2S/SEMT/LM2S/RT/02-034/*A "Thermo-mechanical calculation using CAST3M of CFC tile taking into account a contact heat transfer coefficient between the tile and the dumbbell"*, the thermal heat transfer theory between two solids in contact is described. Two formulations of the heat transfer coefficient were tested for two different thermal fluxes on the tile. In the case of CFC tiles under a weak thermal flux (5 MW.m^{-2}), the use of different thermal contact conductance correlation lead to difference in the maximum Von Mises stress in dumbbell. In the case of high thermal flux, the temperature gradient in the dumbbell remains relatively weak and the Von Mises stress distribution is mainly governed by the force on the centre block.

CONCLUSIONS

RULES FOR DESIGN, FABRICATION AND INSPECTIONS

In fusion reactor components, rupture conditions can be achieved under series of thermal shocks. In the framework of this action, a particular simplified thermal fatigue rule was developed and validated with an associated experimental campaign. Therefore, this activity was mainly focused on the σ_d criterion for pure thermal loading conditions. Thermal fatigue tests are necessary to validate the criterion but such tests were not found in the literature. Part of this action consisted in the design of an experimental set-up that allows realising experiments of thermal fatigue for future application on RAFM steel like 9%Cr material.

In 2002, a thermal fatigue test was performed on a 316L specimen (AFNOR name is Z2 CND 17-12). The specimen is a pipe placed inside a furnace to maintain a hot temperature at its outer surface. A cyclic cooling is imposed by a local cyclic injection of cold water inside the pipe.

A 3D finite element modelling has been introduced to estimate the number of cycles to crack initiation and then the test duration. The application of the σ_d method predicts that, on a pipe having a defect (semi-elliptic defect: depth "a" equal to the 10th of the thickness (a = 1.74 mm), width equal to "8.a"), a crack can initiate in a reasonnable period of time (4748 cycles $\cong$ 16,5 days).

Thermal fatigue tests on RAFM steel (Eurofer) or equivalent 9%Cr material pipes are necessary to validate the criterion for Fusion applications (pure thermal loading conditions).
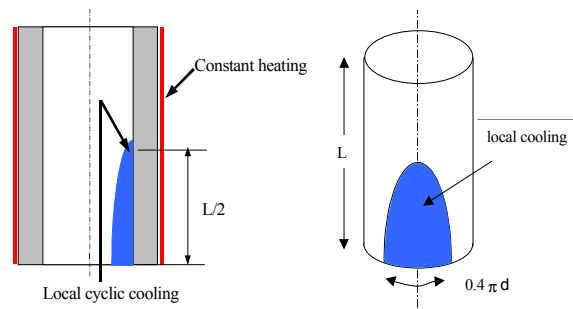
Principle of the test

So, the thermal fatigue test on 316L specimen has to be completed by a future experimental program on RAFM steel like 9%Cr material.

TILES INTEGRITY

Failure criteria for CFC materials can be used to evaluate the integrity of tiles used as plasma facing components under thermal and mechanical loads and to test the different designs.

However rupture strengths must be determine for each type of CFC material. A wide range of CFC materials can be considered for plasma facing components [1]. The mechanical properties (which depend on raw materials, process and structure) are specific to each composite and may differ highly from a composite to another.

For instance, values of the tensile strength reported in literature for CFC composites in the fibres direction ranges from 30 to more than 380 MPa.

The study indicates that two main failure macroscopic failure theories can be used for CFC materials. Values of fracture strength in tension, compression and shear for the different directions (plus eventually interaction terms) must be known to use these criteria.

A complete set of data corresponding to a three dimensional composite [2] has been used to evaluate the integrity of a tile submitted to thermal and mechanical loads.

REFERENCES

[1]   P. G. Valentine et al. Journal of nuclear materials 233-237 (1996) 660-666.

[2]   L. Moncel, 'Etude des mécanismes d'endommagement d'un assemblage cuivre/composite carbone-carbone sous chargement thermomécanique'. Thèse soutenue le 18 Juin 1999. Rapport EUR-CEA-FC-1682.

REPORTS AND PUBLICATIONS

Ph. Matheron, "Progress in the design and construction of a thermal fatigue experimental set-up", CEA report DM2S SEMT/LISN/RT/02-009/A (February, 2002).

Ph. Matheron, "Feasibility of a crack initiation test under thermal fatigue conditions", CEA report DM2S SEMT/LISN/RT/02-031/A (October, 2002).

C. Guerin, "Failure criteria for carbon fibber reinforced carbon composite (CFC)", CEA report DM2S SEMT/LM2S/RT/02-011/A (March, 2002).

C. Guerin, "Evaluation of CFC tile integrity using CAST3M and a Tsai-Wu criterion", CEA report DM2S SEMT/LM2S/RT/02-033/A (October, 2002).

C. Guerin, "Thermo-mechanical calculation using CAST3M of CFC tile taking into account a contact heat transfer coefficient between the tile and the dumbbell", CEA report DM2S SEMT/LM2S/RT/02-034/A (November, 2002).

TASK LEADER

Laetitia NICOLAS

DEN/DM2S/SEMT
CEA Saclay
91191 Gif-sur-Yvette Cedex

Tél. : 33 1 69 08 55 40
Fax : 33 1 69 08 86 84

E-mail : laetitia.nicolas@cea.fr

Not available on line